

Supporting Information

Measurement of cytokine biomarkers using an aptamer -based affinity graphene nanosensor on a flexible substrate toward wearable applications

Zhuang Hao,^{a,b} Ziran Wang,^{a,b} Yijun Li,^a Yibo Zhu,^a Xuejun Wang,^a Carlos Gustavo De Moraes,^c Yunlu Pan,^b Xuezheng Zhao^b and Qiao Lin^{a,*}

^a Department of Mechanical Engineering, Columbia University, New York, NY 10027, USA

^b Department of Mechanical Engineering, Harbin Institute of Technology, Harbin, Heilongjiang 150001, China

^c Department of Ophthalmology, Columbia University, New York, NY 10032, USA

*Corresponding author: qilin@columbia.edu (Qiao Lin)

1 Device Fabrication Protocol

The fabrication protocol was illustrated in Figure S1, the polyethylene naphthalate (PEN) film employed as the substrate of the nanosensor was cleaned successively with acetone, IPA and deionized water, finally dried by N₂ and treated by oxygen plasma.

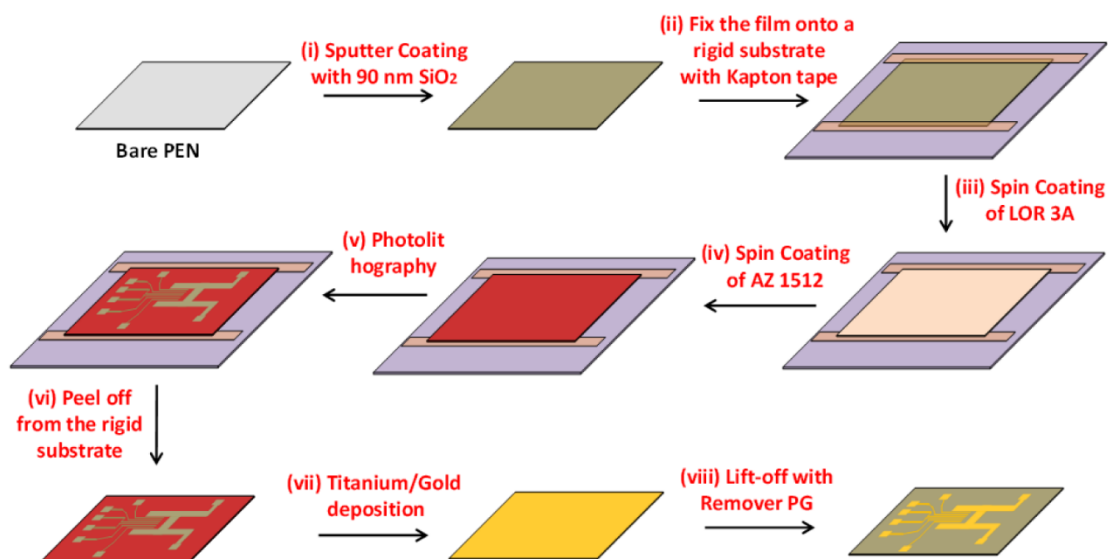


Figure S1 Schematic of the fabrication protocol of a flexible graphene-based field effect transistor (GFET) nanosensor.

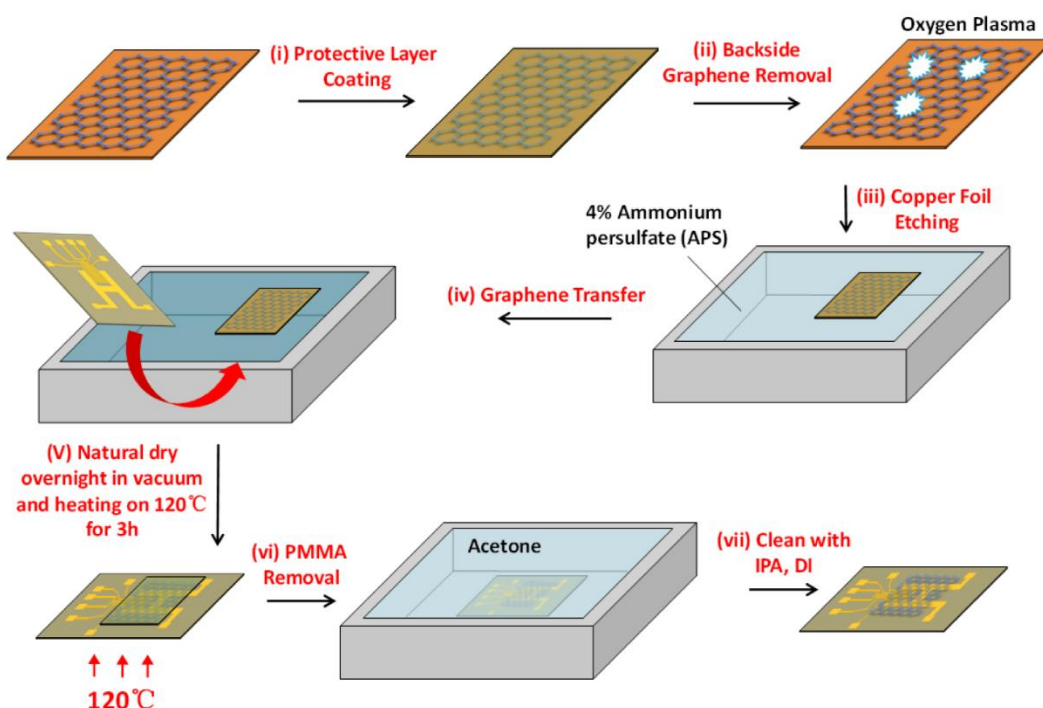


Figure S2 Transfer of monolayer graphene onto arbitrary substrates.

A 50 nm SiO₂ thick nanolayer was subsequently coated on the PEN film using Sputter Deposition System (Orion-8 RF Sputter Deposition System, AJA International

Inc.). Then the flexible substrate was fixed onto a rigid wafer (285 nm SiO₂/Si) using Kapton tape. The nanosensor was fabricated *via* a bilayer lift-off photolithography process. Two layers of resist (sacrificial layer LOR 3A and photoresist AZ 1512) were sequentially spin-coated on the substrate using spin coater (Spin coater Cee Model 200x-F, Brewer Science). The planar source and drain electrodes consisting of a Cr/Au structure (2 nm/43 nm) were defined on the SiO₂ coated PEN using standard photolithography (Mask aligner EVG 620, EVG Group) and metal deposition (Orion-8 E Ebeam Evaporator System, AJA International Inc.) techniques. Then the nanosensor was peeled off and kept in remover PG overnight at room temperature for resist removal. The nanosensor was exposed to oxygen plasma (Plasma Asher Ion 40 plasma etching system, PVA Tepla) to remove the remaining residue on the surface. Finally, the synthesized CVD graphene was then transferred (Figure S2) onto the substrate.

2 Surface Functionalization Protocol

As shown in Figure S3, to immobilize the aptamer VR11 onto the graphene channel, the nanosensor was first immersed in 5 mM 1-Pyrenebutanoic acid succinimidyl ester (PASE) solution for 2 hours at room temperature and sequentially rinsed with pure dimethylformamide (DMF) to remove any free PASE. The nanosensor was then rinsed with 1X PBS followed by incubation with 100 nM aptamer VR11 solution overnight at room temperature. After rinsing with 1X PBS, 100 mM ethanolamine was added into the graphene channel for 1 h to deactivate and block the excess reactive groups remaining on the graphene surface. A polydimethylsiloxane (PDMS)-based open liquid handling chamber (~20 μ L) was used to hold sample solutions and was placed on the top of the nanosensor.

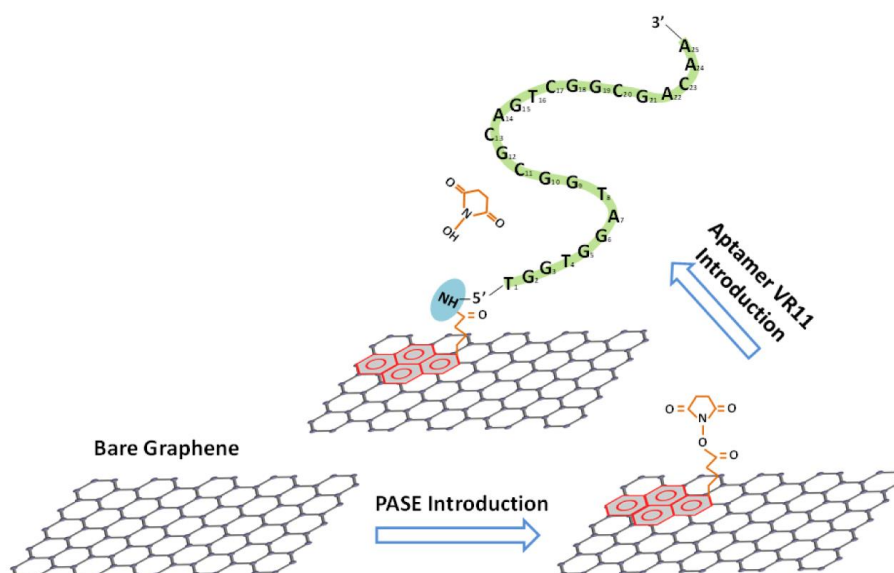


Figure S3. Graphene surface functionalization. PASE stacks on the graphene surface *via* π - π interaction. Aptamer VR11 is connected to the PASE linker through Schiff-base reaction.

3 Characterization of Mechanical Flexibility

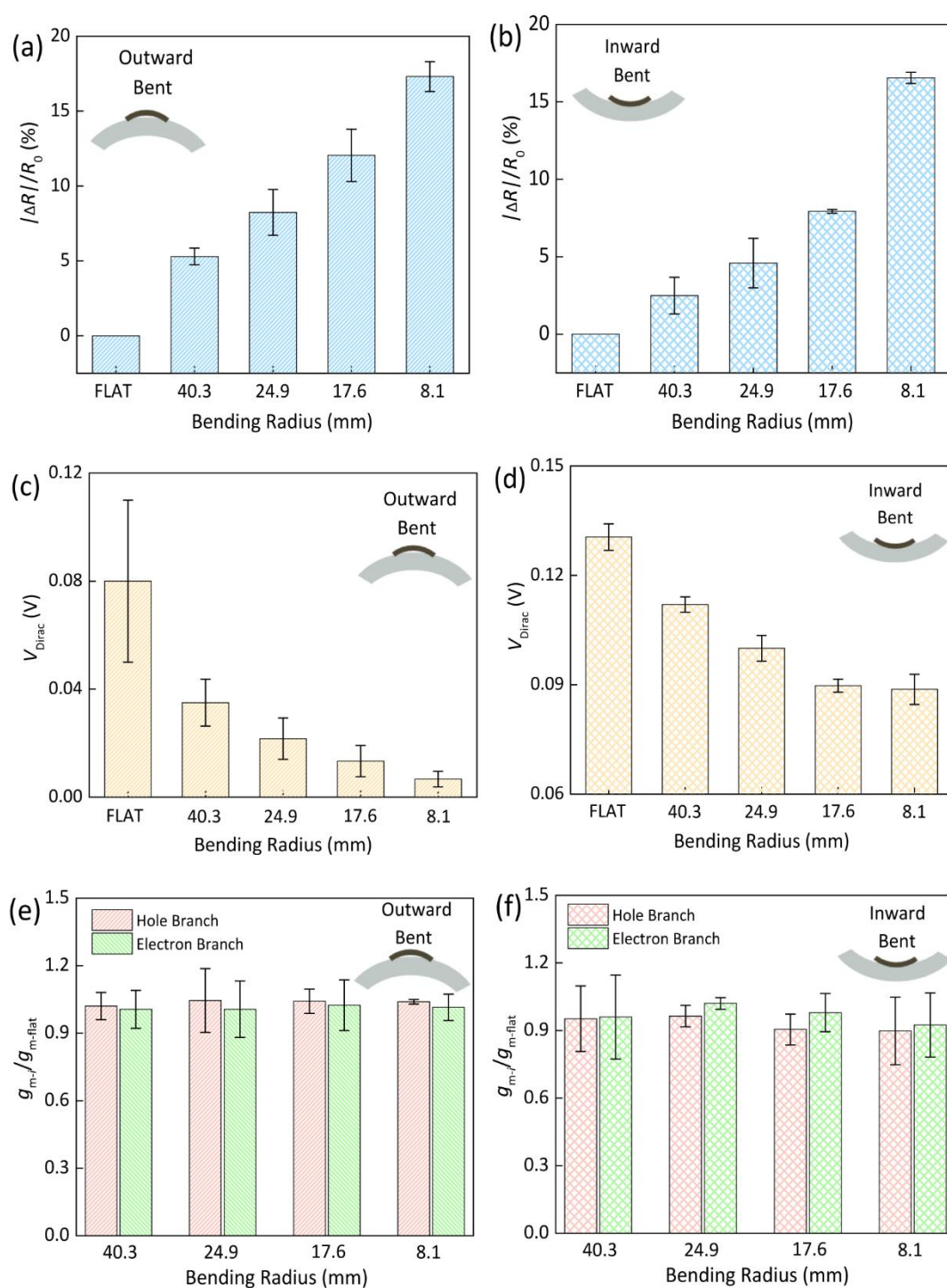


Figure S4 Characterization of graphene electrical properties in bent status. Changes in the resistance (a, b), the Dirac point (c, d) and the transconductance (e, f) of graphene during outward and inward bending process with decreasing bending radii (measured at $V_{ds}=0.001V$).

4 Control Experiment with Untreated Graphene

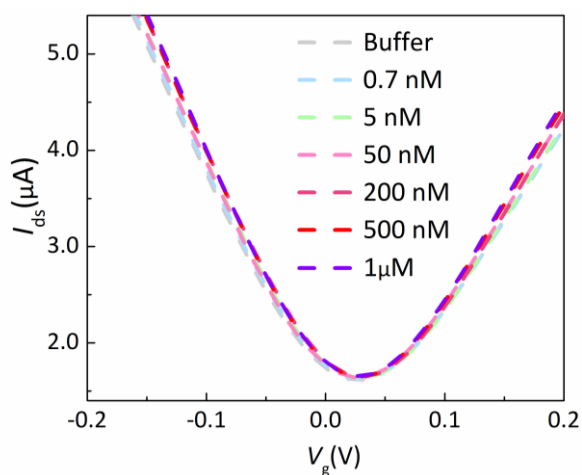


Figure S5 Transfer characteristic curves of bare graphene exposed to the TNF- α (700 pM~1 μ M).

5 Electrical Characterization

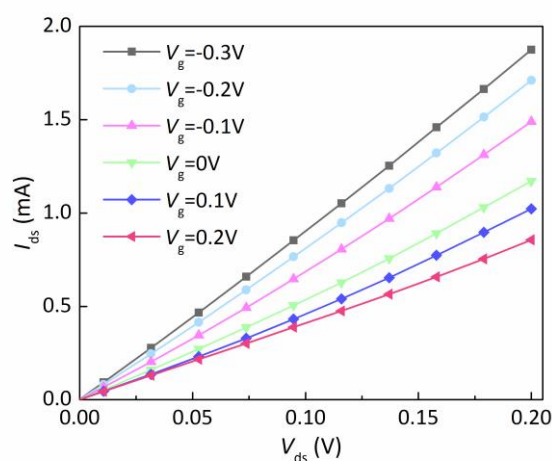


Figure S6 I_{ds} - V_{ds} output characteristics of the nanosensor at different V_g from -0.3~0.2 V in a step of 0.1 V.

6 Data Fitting

The measured $\Delta V_{Dirac}/\Delta V_{Dirac,max}$ ratio was fitted to the Hill-Langmuir equation¹ (Figure 5 b, d, f),

$$\frac{\Delta V_{Dirac}}{\Delta V_{Dirac,max}} = A \frac{\left(\frac{C_{TNF}}{K_D}\right)^n}{1 + \left(\frac{C_{TNF}}{K_D}\right)^n} + A_0 \quad (1)$$

where A is the sensor saturation response when all aptamers are occupied, C_{TNF} is the TNF- α concentration, A_0 is an offset that accounts for the response to the fresh PBS buffer, K_D is the dissociation constant for TNF- α and aptamer VR11 binding, and n is the Hill coefficient

describing the binding cooperativity. A best fitting yields a K_D of 28.4, 27.4 and 28.4 nM at corresponding bending status of flat, outward and inward bending, respectively, A of 1.430, A_0 of -0.02 and n of 0.35.

7 Matrix Condition Studies

To investigate effects of ionic strengths change on the TNF- α detecting capability of our nanosensor, TNF- α detection experiments were conducted in 10 times diluted PBS (13.5 mM Na⁺) and 1X PBS (135 mM Na⁺), respectively. As shown in Figure S7, the normalized device signal, $\Delta V_{\text{Dirac}}/V_{\text{Dirac, max}}$, is plotted as a function of the increasing TNF- α concentration up to 200 nM. It is evident that the maximum variation between normalized signals obtained in different salinity conditions at given concentrations is less than 5.4%, which is insignificant. Similar experimental results are also observed in previous studies.² Consequently, effects of the change in salinity conditions on the normalized response signal of our nanosensor can be ignored.

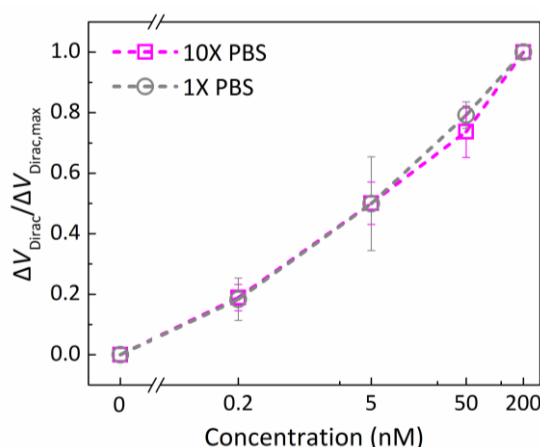


Figure S7. Detection of TNF- α in solutions with different ionic strength conditions (10X or 1X PBS).

To study effects of solution pH changes on the reliability of TNF- α detection, experiments were conducted using TNF- α solutions ranging from 0 to 200 nM with given pH at 6.4, 7.4, and 8.4, respectively. As shown in Figure S8, the normalized device signal $\Delta V_{\text{Dirac}}/V_{\text{Dirac, max}}$, which is measured in different pH solutions, increases monotonically with the ascending TNF- α concentration. Unfortunately, the difference between the normalized signals obtained in 5 nM TNF- α solutions at pH=7.4 and pH=6.4 is over 20%. This is expected, as the aptamer-target binding in general strongly depends on pH.³

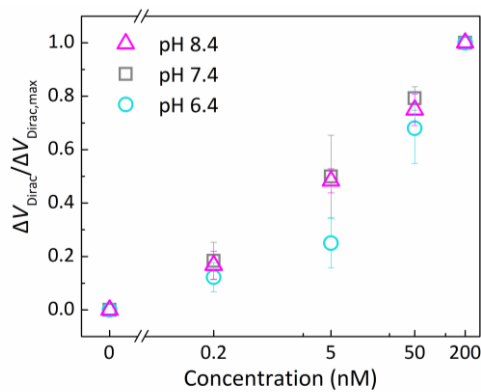


Figure S8. Detection of cytokine TNF- α in solutions with different pH (6.4, 7.4 or 8.4).

Reference

- 1 Y. Zhu, Y. Hao, E. A. Adogla, J. Yan, D. Li, K. Xu, Q. Wang, J. Hone and Q. Lin, *Nanoscale*, 2016, **8**, 5815–5819.
- 2 D. J. Kim, H. C. Park, I. Y. Sohn, J. H. Jung, O. J. Yoon, J. S. Park, M. Y. Yoon and N. E. Lee, *Small*, 2013, **9**, 3352–3360.
- 3 D. J. Kim, I. Y. Sohn, J. H. Jung, O. J. Yoon, N. E. Lee and J. S. Park, *Biosens. Bioelectron.*, 2013, **41**, 621–626.